Nonreciprocal unconventional photon blockade in a driven dissipative cavity with parametric amplification

H. Z. Shen,[1,2,*] Qiu Wang,[1] Jiao Wang,[1] and X. X. Yi[1,2,†]

[1]*Center for Quantum Sciences and School of Physics, Northeast Normal University, Changchun 130024, China*

[2]*Center for Advanced Optoelectronic Functional Materials Research, and Key Laboratory for UV Light-Emitting Materials and Technology of Ministry of Education, Northeast Normal University, Changchun 130024, China*

(Received 9 September 2019; revised manuscript received 19 December 2019; published 22 January 2020)

In this paper, we show that nonreciprocal unconventional photon blockade can be observed in a spinning cavity immersed in a degenerate optical parametric amplifier (OPA) driven by the laser driving with weak Kerr nonlinearities through the Fizeau drag. We analytically derive the optimal conditions for strong antibunching, which are in good agreement with those obtained by numerical simulations. Under the weak driving condition, we discuss the physical origins of the nonreciprocal unconventional photon blockade, which originates from the destructive interference between different paths from the ground state to two-photon states by driving the device from the left side. While the quantum interference paths are broken when the device is driven from the right side, which leads to the occurring of the photon bunching. Moreover, we extend the above results to the general non-Markovian regimes, in which the cavity couples with a thermal reservoir consisting of collection of infinite oscillators (bosonic photonic modes). We show nonreciprocal unconventional photon blockade exhibits a transition from the non-Markovian to Markovian regimes by controlling environmental spectral width regardless of the weakness of OPA gain and driving field.

DOI: 10.1103/PhysRevA.101.013826

I. INTRODUCTION

The photon blockade effect (PB) is one of the mechanisms for achieving single photon sources, which plays an important role in quantum metrology [1] and quantum information technologies [2,3], where the strong photon antibunching is required. PB is a phenomenon that a single photon in a nonlinear medium blocks the transmission of a second photon [4], which is one of the mechanisms for creating strong antibunching photons. The PB has attracted significant experimental and theoretical attentions recently, because there is a crucial requirement for the generation and manipulation of a single photon in information and communication technology. The general idea to realize this source is to find systems able to produce sub-Poissonian light when it is driven by a classical light field.

There are currently two methods to realize photon blockade. The first method is known as conventional photon blockade (CPB) and the observation of antibunching requires large nonlinearities with respect to the decay rate of the system. The CPB was first observed in an optical cavity coupled to a single trapped atom [5]. Subsequently, strong antibunching behaviors were observed in different systems by a sequence of experimental groups, including a quantum dot in a photonic crystal system [6], circuit cavity quantum electrodynamics systems [7–22], and circuit QED [23,24]. The theoretical models about CPB include quantum optomechanical system [25–39], exciting polaritons [40], two-level system coupled to the cavity [41–44], dynamical blockade [45], quantum dot coupled to a nanophotonic waveguide [46], and four-level quantum emitter [47]. Many schemes have been completed in nanostructured cavities and semiconductor microcavities with second-order nonlinearity [48–50]. The potential applications of photon-blockade include the realization of interferometers [51], quantum nonreciprocity [52,53], and single-photon transistors [54].

Another independent method is proposed by Liew and Savona, where strong photon antibunching can be obtained when nonlinearities are smaller than the decay rates of the cavity modes [55]. This mechanism is called unconventional photon blockade (UPB), sometimes UPB is also referred to as weak nonlinear PB. This feature can be understood as destructive quantum interference between distinct driven-dissipative pathways [56–59]. Very recently, based on this mechanism, the anomalous photon blockade effect in the microwave domain has been observed in coupled superconducting resonators [60], and quantum dot cavity-QED [61] in experiment. Based on this fundamental principle, many quantum systems are predicted to have photon blockade effect with weak nonlinearities, such as the nonlinear photonic molecule [57,62,63], bimodal coupled polaritonic cavities [64], optical cavity with a quantum dot [65–67], coupled single-mode cavities with second- or third-order nonlinearity [68–76], coupled optomechanical system [77,78], semiconductor cavity [79], a gain cavity [80], and Gaussian squeezed states [81–83].

While nonreciprocal photon blockade [84], which break the physical symmetry, allowing light to propagate from one side but not the other side, also plays a very important role

*shenhz458@nenu.edu.cn
†yixx@nenu.edu.cn

in a wide range of applications, such as signal processing and invisible sensing [85]. Due to this special property, it has applications in many aspects, such as isolators [86,87] and circulators [88]. Moreover, it has been realized in optomechanical systems [89–95], Kerr resonators [96–99], thermo systems [100–102], second-order nonlinearity system [103], coupled cavities [104], devices with temporal modulation [105], and non-Hermitian systems [106–108]. Besides, nonreciprocal quantum amplifiers have been explored recently [109–111], which might have unique applications in chiral quantum technologies and topological photonics [112].

Here we study nonreciprocal unconventional photon blockade in a spinning cavity coupled respectively with degenerate optical parametric amplifier (OPA) and laser driving through the Fizeau drag. We find that, by spinning a resonator, unconventional photon blockade can emerge in a nonreciprocal way for the clockwise (CW) or counterclockwise (CCW) modes even with weak OPA strength; that is, strongly antibunched photons can emerge only by driving the device from left side, but not the right side. We show that this nonreciprocal unconventional photon blockade originates from the destructive quantum interference between two paths which are formed by the OPA pump and a driving field. We analytically derive an optimal condition for strong photon antibunching, which is in good agreement with that obtained by the full numerical simulation. The presented results then are expanded to the non-Markovian regimes and compared with Markovian approximation in the weak-coupling limit.

The remainder of the paper is organized as follows. In Sec. II, we introduce a model to describe the studied system consisting of the spinning cavity coupled with degenerate optical parametric amplifier (OPA) and laser driving, respectively. In Sec. III, we give the optimal conditions for nonreciprocal unconventional photon blockade in this system and discuss the origin of the nonreciprocal unconventional photon blockade. In Sec. IV, we calculate analytically the equal-time second-order correlation function and compare it with the result from numerical simulation with the master equation under Markovian approximation. In Sec. V, we extend nonreciprocal unconventional photon blockade in driven cavity with parametric interactions to non-Markovian bath and compare it with that in the Markovian regime. In Sec. VI, we present some discussions on the experimental implementation of this scheme. The conclusions and discussions are given in Sec. VII.

II. MODEL HAMILTONIAN

We consider a rotating optical cavity to realize the nonreciprocal photon blockade effects in general environments with single- and two-photon drivings. The cavity rotates with a fixed angular velocity Ω and an external classical light is coupled into and out of the cavity, which is sketched in Fig. 1. The total Hamiltonian without the dissipation is given by (Setting $\hbar = 1$)

$$\hat{H}_S(t) = (\omega_c + \Delta_F)\hat{a}^\dagger\hat{a} + [F(t)\hat{a}^\dagger + G(t)\hat{a}^{\dagger 2} + \text{H.c.}], \quad (1)$$

where H.c. stands for the Hermitian conjugate. The single-photon driving is $F(t) = Fe^{-i\omega_l t}$ via the frequency ω_l with $F = fe^{-i\phi}$, and two-photon pumping is $G(t) = Ge^{-i\omega_p t}$ via

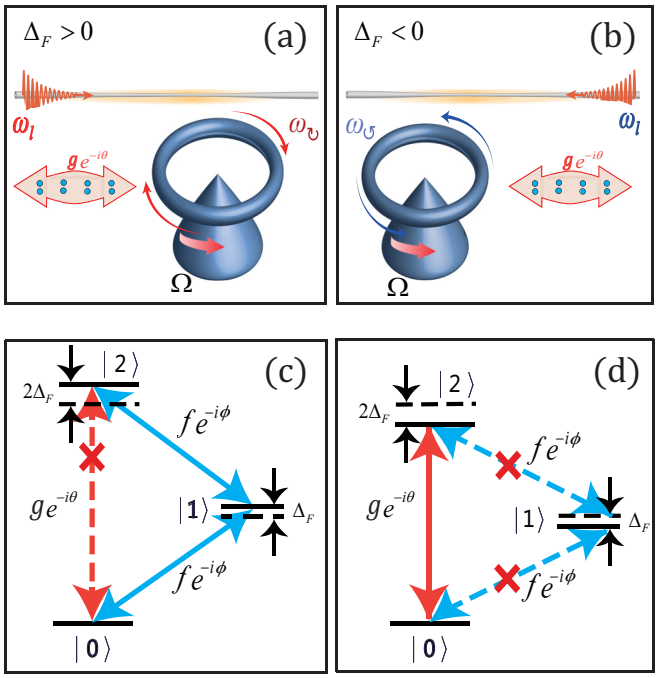

FIG. 1. A nonreciprocal photon blockade can be realized in a spinning cavity coupled with a degenerate optical parametric amplifier (OPA) [12,58,81,83,113–120]. Spinning the resonator results in different Sagnac-Fizeau shifts Δ_F for controlling CW or CCW optical mode experiencing different refractive indices with an angular velocity Ω. (a) Indicates driving the device from the left side ($\Delta_F > 0$), which thereafter is denoted by L, while (b) indicates driving the cavity from the right side ($\Delta_F < 0$), which thereafter is denoted by R. With the Sagnac-Fizeau shifts, photon blockade or photon-induced tunneling can be observed by driving the spinning resonator from one side, but not from the other side. (c) By driving the system from the left side, the direct excitation from state $|0\rangle$ to state $|2\rangle$ (red dashed arrow) will be forbidden by destructive quantum interference with the other paths drawn by blue arrows, which leads to photon antibunching. (d) Photon bunching occurs by driving the system from the right side, due to the lack of the complete destructive quantum interference between the indicated levels (drawn by crossed blue dashed arrows).

the two-photon frequency $\omega_p = 2\omega_c$ with $G = ge^{-i\theta}$. $\hat{a}$ and $\hat{a}^\dagger$ are, respectively, the annihilation and creation operators for photons inside the optical cavity. ω_c is the cavity-mode frequency of nonspinning cavity. The cavity mode experiences a Fizeau shift because of the rotation, hence we have $\omega_c \to \omega_c + \Delta_F$. Δ_F here is decided by the fixed angular velocity of the rotating cavity according to [121–123]

$$\Delta_F = \pm\frac{nr\Omega\omega}{c}\left(1 - \frac{1}{n^2} - \frac{\lambda}{n}\frac{dn}{d\lambda}\right) \equiv \beta\Omega, \quad (2)$$

where n is the refractive index. r is the cavity radius. c is the speed of light in vacuum, and λ is the wavelength of the external classical light. Here, we fix the CCW rotation of the resonator, hence $\Delta_F > 0$ ($\Delta_F < 0$) means that the light propagates against (along) the direction of the rotating cavity as shown in Fig. 1(a) [Fig. 1(b)], i.e., the CW and CCW mode frequencies are $\omega_c \pm |\Delta_F|$, respectively.

In the following, we will consider the quantum system coupled to the kth mode (eigenfrequency ω_k) of the environment via the system annihilation (creation) operator. In a rotating frame defined by $U(t) = \exp[-i\omega_l t(\hat{a}^\dagger\hat{a} + \sum_k b_k^\dagger b_k)]$, the total Hamiltonian is transformed to a time-independent one as follows:

$$\hat{H} = (\Delta_l + \Delta_F)\hat{a}^\dagger\hat{a} + G\hat{a}^{\dagger 2} + G^*\hat{a}^2 + F\hat{a}^\dagger + F^*\hat{a} + \sum_k \Omega_k \hat{b}_k^\dagger \hat{b}_k + \sum_k v_k(\hat{a}\hat{b}_k^\dagger + \hat{b}_k\hat{a}^\dagger), \quad (3)$$

where $\Delta_l = \omega_c - \omega_l$ and $\Omega_k = \omega_k - \omega_l$ denote the detunings of the optical cavity and kth mode (eigenfrequency ω_k) of the environment from the driving field. Here $\hat{b}_k$ ($\hat{b}_k^\dagger$) is the annihilation (creation) operator, and v_k is coupling coefficient between system and environment, respectively.

III. NONRECIPROCAL UNCONVENTIONAL PHOTON BLOCKADE UNDER MARKOVIAN APPROXIMATION

Based on the bilinear operator characteristics of the open quantum system, we can derive the general master equation with the OPA pump and the Fizeau-Sagnac drag by Heisenberg-Langevin equation. For this purpose, we below use the Heisenberg picture approach to solve the dynamics of the cavity coupled with the reservoir. The time evolutions of the cavity annihilation operator $\hat{a}(t) = U^\dagger(t)\hat{a}(0)U(t)$ and the reservoir operator $\hat{b}_k(t) = U^\dagger(t)\hat{b}_k(0)U(t)$ satisfy Heisenberg equation, where $U(t) = e^{-i\hat{H}t}$ with $\hat{H}$ given by Eq. (3). Through simple calculations and the use of Hamiltonian Eq. (3), we obtain an integrodifferential equation for the cavity field operator $\hat{a}(t)$,

$$\frac{d}{dt}\hat{a}(t) = -i(\Delta_l + \Delta_F)\hat{a}(t) - 2iG\hat{a}^\dagger - iF - i\hat{\mathcal{R}}(t) - \int_0^t d\tau[\hat{a}(\tau)C(t-\tau)], \quad (4)$$

where the external driven environment operator $\hat{\mathcal{R}}(t) = \sum_k v_k\hat{b}_k(0)e^{-i\Omega_k t}$, and the correlation function,

$$C(t) = \sum_k v_k^2 e^{-i\Omega_k t} \equiv \int e^{-i(\omega-\omega_l)t}J(\omega)d\omega, \quad (5)$$

where $J(\omega) = \sum_k v_k^2\delta(\omega - \omega_k)$ denotes the spectral density of the environment. The optical cavity field operator $\hat{a}(t)$ can be expressed as a combination of the initial field operators $\hat{a}(0)$ and $\hat{b}_k(0)$ due to the linearity of Eq. (4),

$$\hat{a}(t) = \mathcal{X}(t)\hat{a}(0) + \mathcal{Y}(t)\hat{a}^\dagger(0) + \hat{\mathcal{Z}}(t). \quad (6)$$

The time-dependent functions $\mathcal{X}(t)$, $\mathcal{Y}(t)$, and operator $\hat{\mathcal{Z}}(t)$ can be determined by substituting Eq. (6) into Eq. (4) and comparing coefficients of the initial system operators, we have

$$\begin{aligned}
\dot{\mathcal{X}}(t) &= -i(\Delta_l+\Delta_F)\mathcal{X}(t) - 2iG\mathcal{Y}^*(t) - \int_0^t d\tau C(t-\tau)\mathcal{X}(\tau),\\
\dot{\mathcal{Y}}(t) &= -i(\Delta_l+\Delta_F)\mathcal{Y}(t) - 2iG\mathcal{X}^*(t) - \int_0^t d\tau C(t-\tau)\mathcal{Y}(\tau),\\
\dot{\hat{\mathcal{Z}}}(t) &= -i(\Delta_l+\Delta_F)\hat{\mathcal{Z}}(t) - 2iG\hat{\mathcal{Z}}^\dagger(t) - \int_0^t d\tau C(t-\tau)\hat{\mathcal{Z}}(\tau) - iF - i\hat{\mathcal{R}}(t),
\end{aligned} \quad (7)$$

with the initial values $\mathcal{X}(0) = 1$, $\mathcal{Y}(0) = 0$, and $\hat{\mathcal{Z}}(0) = 0$. The integrodifferential equations in Eq. (7) show that $\mathcal{X}(t)$ and $\mathcal{Y}(t)$ are the propagating functions of the optical cavity. Inhomogeneous environment operator $\hat{\mathcal{Z}}(t)$ can be obtained analytically from Eq. (7) by the Laplace transformation methods as follows:

$$\hat{\mathcal{Z}}(t) = \hat{\sigma}(t) + \mu(t), \quad (8)$$

where the contributions induced by the environment and driving field, respectively, are

$$\begin{aligned}
\hat{\sigma}(t) &= i\int_0^t d\tau[\mathcal{Y}(\mathrm{t}-\tau)\hat{\mathcal{R}}^\dagger(\tau) - \mathcal{X}(\mathrm{t}-\tau)\hat{\mathcal{R}}(\tau)],\\
\mu(t) &= i\int_0^t d\tau[\mathcal{Y}(\mathrm{t}-\tau)F^* - \mathcal{X}(\mathrm{t}-\tau)F].
\end{aligned} \quad (9)$$

Now we assume that the system undergoes a Gaussian Ornstein-Uhlenbeck process (corresponding to the Lorentzian spectrum density) [124–126] described by

$$C(t-t') = \tfrac{1}{2}\gamma\lambda e^{-\lambda|t-t'|}, \quad (10)$$

where the parameter λ defines the spectral width of the reservoir and is connected to the reservoir correlation time $\tau_r = \lambda^{-1}$. The parameter γ can be shown to be related to the decay of the system in the Markovian limit with a flat spectrum. The relaxation time scale is $\tau_l = \gamma^{-1}$.

In many physical systems described by the Hamiltonian of Eq. (3), the Markovian approximation for open systems [127,128] is valid, where the coupling strength between the system and the environment is very weak and the characteristic correlation time τ_r of the environment is sufficiently shorter than that τ_l of the system (i.e., $\lambda \gg \gamma$), a procedure which is known as the Markovian approximation:

$$\tau_r \ll \tau_l, \quad (11)$$

or, equivalently, the spectrum of the reservoir takes the value $J(\omega) = \frac{\gamma}{2\pi}$, which leads to a Markovian dynamics. The reservoir has no memory effect on the evolution of the system. Then, according to Eq. (5) or Eq. (10), we have

$$C(t-t) = \gamma\delta(t-t), \quad (12)$$

where $\delta(t)$ denotes the Dirac delta function. With these results, we can easily obtain the master equation for the system in Markovian approximation [12,58,81,83,113–120]

$$\dot{\rho} = -i[\hat{H}_{\mathrm{Mar}}, \rho] + \gamma\left(\hat{a}\rho\hat{a}^\dagger - \frac{1}{2}\hat{a}^\dagger\hat{a}\rho - \frac{1}{2}\rho\hat{a}^\dagger\hat{a}\right), \quad (13)$$

where $\hat{H}_{\mathrm{Mar}} = (\Delta_l + \Delta_F)\hat{a}^\dagger\hat{a} + G\hat{a}^{\dagger 2} + G^*\hat{a}^2 + F\hat{a}^\dagger + F^*\hat{a}$.

Now we focus on the statistic properties of photons in cavity, which can be described by the equal-time second-order correlation function,

$$g^{(2)}(0) = \frac{\langle\hat{a}^{\dagger 2}\hat{a}^2\rangle}{\langle\hat{a}^\dagger\hat{a}\rangle^2}. \quad (14)$$

We know that $g^{(2)}(0) < 1$ means single-photon blockade. In Fig. 2(a), we show the equal-time second-order correlation

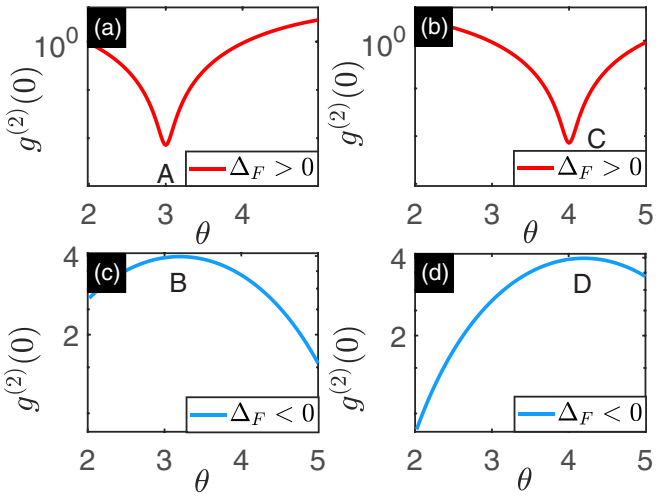

FIG. 2. The second-order correlation function $g^{(2)}(0)$ versus the phase θ (The unit of θ is rad) in two-photo pumping for different input directions. Here and hereafter, Δ_l, Δ_F, G, F, and λ are rescaled in units of γ, and t is then in units of $1/\gamma$. Hence, all parameters are dimensionless. (a) At $f = 0.1504\gamma$, $\phi = 1.5498$rad, single-photon blockade in Fig. 2(a) or photon bunching in Fig. 2(c) occurs at $\theta =$ 3rad by driving the device from the left or right side, with the same strength. At $f = 0.1504\gamma$, $\phi = 2.0498$rad, single-photon blockade in Fig. 2(b) or photon bunching in Fig. 2(d) occurs at $\theta = 4$rad by driving the device from the left or right side, with the same strength. The other parameters chosen are $\Delta_l = 0$, $g = 0.0045\gamma$, and $|\Delta_F| = 5\gamma$.

function $g^{(2)}(0)$ as a function of the phase θ in two-photon pumping. The figures are plotted in the weak driving limit. Interesting features can be found at $\theta = 3$rad and $\theta = 4$rad, marked, respectively, by A, B, C, and D. These points correspond to different physical phenomena. When the phase is $\theta = 3$rad, we have interesting observations that the equal-time second-order correlation function is less than one at point A (corresponding to single-photon blockade) when the laser drives the cavity from the left side, and greater than one at point B (corresponding to photon bunching) when the cavity is driven from the right side. If we change the laser phase ϕ and tune it to make $\phi = 2.0498$rad, then the similar observations at $\theta = 4$rad can be found in Figs. 2(b) and 2(d). This suggests that the nonreciprocal unconventional photon blockade effect can be observed with very weak nonlinearity $g \ll \gamma$.

To gain more insights into the nonreciprocal unconventional single-photon blockade shown in Figs. 1 and 2, we develop an approximately analytical expression for the system by considering only the three lowest levels in Figs. 1(c) and 1(d). Assume that the system is initially prepared in $|0\rangle$, and only these levels are occupied due to the driving, the state of the system can be written as [30,57]

$$|\Phi\rangle = B_0|0\rangle + B_1|1\rangle + B_2|2\rangle, \tag{15}$$

where B_j is time-dependent function denoting the probability amplitude on the cavity photon state $|j\rangle$. Taking $\hat{H}_{\rm eff} = \hat{H}_{\rm Mar} - i\gamma\hat{a}^\dagger\hat{a}/2$ as the effective Hamiltonian for the system and substituting $|\Phi\rangle$ into the Schrödinger equation $i\frac{\partial}{\partial t}|\Phi\rangle = \hat{H}_{\rm eff}|\Phi\rangle$, we obtain a set of equations for B_j,

$$\begin{aligned} i\dot{B}_0 &= F^*B_1 + \sqrt{2}G^*B_2, \\ i\dot{B}_1 &= FB_0 + \tilde{\Delta}B_1 + \sqrt{2}F^*B_2, \\ i\dot{B}_2 &= \sqrt{2}GB_0 + \sqrt{2}FB_1 + 2\tilde{\Delta}B_2, \end{aligned} \tag{16}$$

where $\tilde{\Delta} = \Delta_l + \Delta_F - i\gamma/2$. Under the weak driving condition, we have $|B_0| \gg |B_1|, |B_2|$. In steady state, $\frac{\partial}{\partial t}B_j = 0$. Noticing Eq. (14), the conditions for $g^{(2)}(0) \to 0$ are derived from Eq. (16) by setting $B_2 = 0$, so we arrive at

$$F\bar{B}_0 + \tilde{\Delta}\bar{B}_1 = 0, \quad \sqrt{2}G\bar{B}_0 + \sqrt{2}F\bar{B}_1 = 0, \tag{17}$$

where $\bar{B}_j$ denotes the steady probability amplitude of B_j. Based on the optimal equations, we can obtain the optimal parameters as follows:

$$f_{\rm opt} = \frac{\sqrt{g}[\gamma^2 + 4(\Delta_l + \Delta_F)^2]^{1/4}}{\sqrt{2}}, \tag{18}$$

$$\phi_{\rm opt} = \begin{cases} z, & 2(\Delta_l + \Delta_F)\cos\theta - \gamma\sin\theta > 0, \\ z + \frac{1}{2}\pi, & 2(\Delta_l + \Delta_F)\cos\theta - \gamma\sin\theta < 0, \end{cases} \tag{19}$$

where $z = \frac{1}{2}\arctan[\frac{\gamma\cos\theta + 2(\Delta_l+\Delta_F)\sin\theta}{2(\Delta_l+\Delta_F)\cos\theta - \gamma\sin\theta}]$. We should point out that when the optimal condition Eqs. (18) and (19) are simultaneously satisfied, strong antibunching can be obtained; otherwise, the system is not in strong antibunching regimes.

We will use the optimal conditions given by Eqs. (18) and (19) to understand the extreme points shown in Fig. 2. In Figs. 2(a) and 2(c), when $\Delta_l = 0$, $g = 0.0045\gamma$, $|\Delta_F| = 5\gamma$, $\theta = 3$rad we have the optimal values $f = 0.1504\gamma$, $\phi = 1.5498$rad, which are consistent with those given by Eqs. (18) and (19), this explains the points A and B in Fig. 2. When we change θ to 4rad, we have the optimal values $f = 0.1504\gamma$, $\phi = 2.0498$rad which are given by Eqs. (18) and (19), this explains what we find at points C and D.

Although the optimal values can be found by numerically solving the master equation, the analytical optimal values given by the effective Hamiltonian have the following advantages. First, the analytical optimal f and ϕ given by Eqs. (18) and (19) are convenient to analyze the regime of antibunching, this would help in experiments find the required parameters. Secondly, by the analytical expressions for $f_{\rm opt}$ and $\phi_{\rm opt}$, we can find that the roles the system parameters play.

In Figs. 1(c) and 1(d), we show the energy levels and the transition paths. The physical origin of strong photon antibunching is the destructive interference between direct and indirect paths of two-photon excitations, i.e.,

$$|0\rangle \xrightarrow{\sqrt{2}ge^{-i\theta}} |2\rangle, \quad |0\rangle \xrightarrow{fe^{-i\phi}} |1\rangle \xrightarrow{\sqrt{2}fe^{-i\phi}} |2\rangle. \tag{20}$$

For spinning cavity with OPA and dissipation driven by the laser driving, $g^{(2)}(0)$ exhibits giant nonreciprocity, which can be seen in Fig. 2(a). The photon blockade can be generated, i.e., $g^{(2)}(0) \sim 0.0072$ for $\Delta_{\rm F} > 0$, while significantly suppressed, i.e., $g^{(2)}(0) \sim 3.94$ for $\Delta_{\rm F} < 0$, which can be seen more clearly in Fig. 2(c). The nonreciprocal unconventional photon blockade induced by Fizeau light-dragging effect, with

up to two orders of magnitude difference of $g^{(2)}(0)$ for opposite directions, can be achieved even with a weak nonlinearity. Furthermore, in Figs. 2(b) and 2(d) with $\phi = 2.0498$rad, the similar phenomena can be observed. This can be explained in Fig. 1. In Fig. 1(c), by driving the system from the left-hand side, the direct excitation from state $|0\rangle$ to state $|2\rangle$ will be forbidden by the destructive quantum interference between the indirect paths of two-photon excitations, which leads to photon antibunching. In contrast, photon bunching occurs by driving the system from the right side due to the lack of the complete destructive quantum interference between the indicated levels [see Fig. 1(d)].

IV. ANALYTICAL EXPRESSIONS FOR THE SECOND-ORDER CORRELATION FUNCTION

In this section, we will derive an analytical expression for the second-order correlation function and compare it with the full numerical simulation by solving master Eq. (13). To approximately obtain the analytical solution of the second-order correlation function $g^{(2)}(0)$, we need estimate Eq. (13). Moreover, in the weak driving limit, we have $|B_0| \gg |B_1|, |B_2|$ and assume that the vacuum state is approximately occupied with $B_0 = 1$ in Eq. (16). The second-order correlation function is calculated by the steady-state solutions of Eq. (16). We set the time derivatives to zero and solve the equations iteratively, order by order, in the weak driving limit. Finally, we obtain the steady-state probability amplitude equations

$$\begin{aligned} F + \tilde{\Delta}\bar{B}_1 + \sqrt{2}F^*\bar{B}_2 &= 0, \\ \sqrt{2}G + \sqrt{2}F\bar{B}_1 + 2\tilde{\Delta}\bar{B}_2 &= 0, \end{aligned} \tag{21}$$

which lead to

$$\begin{aligned} \bar{B}_1 &= -\frac{2f\{2ge^{2i\phi} + e^{i\theta}[i\gamma - 2(\Delta_l + \Delta_F)]\}}{e^{i(\theta+\phi)}\{4f^2 + [\gamma + 2i(\Delta_l + \Delta_F)]^2\}}, \\ \bar{B}_2 &= \frac{\sqrt{2}\{e^{2i\phi}g[\gamma + 2i(\Delta_l + \Delta_F)] - 2ie^{i\theta}f^2\}}{ie^{i(\theta+2\phi)}\{4f^2 + [\gamma + 2i(\Delta_l + \Delta_F)]^2\}}. \end{aligned} \tag{22}$$

Therefore, considering the total state Eq. (15), we can obtain the analytical expression of the second-order correlation function

$$g^{(2)}(0) = \frac{\langle \hat{a}^{\dagger 2}\hat{a}^2\rangle}{\langle \hat{a}^\dagger \hat{a}\rangle^2} \simeq \frac{2|\bar{B}_2^2|}{|\bar{B}_1^4|}, \tag{23}$$

where $\bar{B}_1$ and $\bar{B}_2$ are given by Eq. (22). To compare the analytical solution with the full numerical solution of the second-order correlation function $g^{(2)}(0)$, we plot the second-order correlation function $g^{(2)}(0)$ as a function of the phase θ in Fig. 3. The red-circle lines indicate the full numerical simulations by solving master Eq. (13), and the blue-square lines correspond to the analytical results Eq. (23). We find that the analytical results of the second-order correlation function show good agreement with those obtained by the full numerical simulations.

Our analytical method is developed to find the optimal parameters $(f_{\rm opt}, \phi_{\rm opt})$ that minimize the second-order correlation function where a truncation of the Hilbert space to 2 photons is used. Thus the analytical solution of the second-order correlation function is inaccurate when the photon number is large. However, as seen in Fig. 3, the optimal value is the same as that from the numerical solution, demonstrating the feasibility of our analytical method.

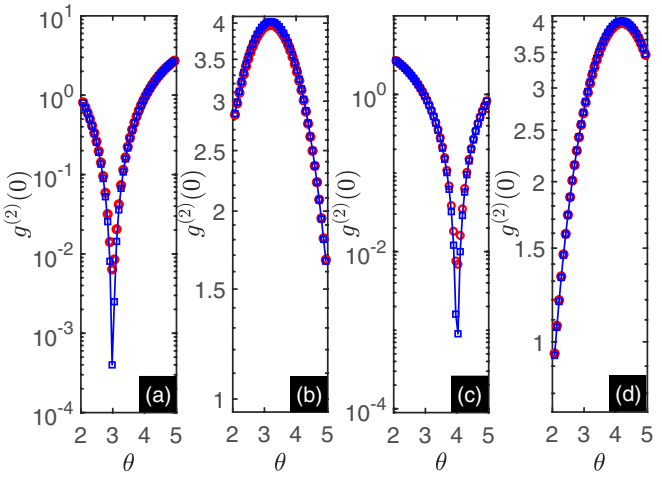

FIG. 3. This figure indicates that the optimal value given by the analytical method is consistent with that given by numerical simulation (The unit of θ is rad). The blue-square and red-circle lines denote $g^{(2)}(0)$ for the analytical expression given by Eq. (23) and full numerical simulation by solving the master Eq. (13), respectively. The parameters chosen are the same as those in Fig. 2.

From Fig. 3, we observe that the second-order correlation function $g^{(2)}(0)$ can arrive at $10^{-5} \sim 10^{-4}$ orders of magnitude at optimal points, whereas the analytical results can reach 10^{-15} orders of magnitude (very close to zero). The reason leading to this difference is that the Hilbert space is truncated into the finite dimension in the analytical derivation. On the other hand, when we substitute the optimal conditions given by Eqs. (18) and (19) into the analytical solution of $g^{(2)}(0)$ in Eq. (23), we find $g^{(2)}(0) = 0$ or $\bar{B}_2 = 0$, as predicted. However, in the numerical calculation for $g^{(2)}(0)$, the state $|3\rangle$ ($\bar{B}_3$) is actually occupied with very small probability in the weak driving limit, which has been ignored in the analytical analysis. Overall, we do not take the state $|3\rangle$ (or the higher state $|n\rangle$ for $n > 3$) into account in Eq. (15). This is the essential reason of leading to the difference between the analytical results and the numerical simulations for $g^{(2)}(0)$.

V. NONRECIPROCAL UNCONVENTIONAL PHOTON BLOCKADE WITH NON-MARKOVIAN EFFECTS

To give the non-Markovian master equation of the system to be investigated, we assume that the system and environment are initially in an uncorrelated state-reservoir modelled by Hamiltonian $\hat{H}_R = \sum_k \omega_k \hat{b}_k^\dagger \hat{b}_k$, which is in a thermal equilibrium state as follows:

$$\rho_{SR}(0) = \rho(0) \otimes \rho_R(0), \quad \rho_R(0) = \frac{e^{-\beta \hat{H}_R}}{{\rm Tr}_R e^{-\beta \hat{H}_R}}. \tag{24}$$

The factorized initial density matrix Eq. (24) guarantees that the Liouville operator is independent of initial system state, which is also observed in the quantum Brownian particle [129–132], quantum two-level systems in various materials [133–137], quantum cavity systems coupled to

structured environments, and general non-Markovian environments [138–141]. The integral kernels (both of which are of Gaussian form and result from the linearity of total Hamiltonian) make the reduced density matrix $\rho(t) = \mathrm{Tr}_R[\rho_{SR}(t)]$ also a Gaussian. Together with the requirements of conservation of probability [$\mathrm{Tr}(\dot{\rho}) = 0$], hermiticity ($\rho = \rho^\dagger$), and state-independent coefficients, we obtain the following form of time-convolutionless master equation:

$$\begin{aligned}\dot{\rho} =& -i[\hat{\mathcal{H}}(t), \rho] \\ &+ \gamma_1(t)(2\hat{a}\rho\hat{a}^\dagger - \hat{a}^\dagger\hat{a}\rho - \rho\hat{a}^\dagger\hat{a}) \\ &+ \gamma_2(t)(\hat{a}\rho\hat{a}^\dagger + \hat{a}^\dagger\rho\hat{a} - \hat{a}^\dagger\hat{a}\rho - \rho\hat{a}\hat{a}^\dagger) \\ &+ [\gamma_3^*(t)(2\hat{a}\rho\hat{a} - \hat{a}\hat{a}\rho - \rho\hat{a}\hat{a}) + \mathrm{H.c.}], \end{aligned} \tag{25}$$

with the time-dependent effective Hamiltonian

$$\hat{\mathcal{H}}(t) = \mathcal{E}(t)\hat{a}^\dagger\hat{a} + \mathcal{S}(t)\hat{a}^{\dagger 2} + \mathcal{S}^*(t)\hat{a}^2 + \chi(t)\hat{a}^\dagger + \chi^*(t)\hat{a}, \tag{26}$$

where the time-dependent parameter $\mathcal{E}(t)$ is the optical cavity energy induced by the OPA pump and non-Markovian environment. $\mathcal{S}(t)$ denotes the two-photon process produced by the OPA pump. $\gamma_1(t)$, $\gamma_2(t)$, and $\gamma_3(t)$ usually are, respectively, the dissipative, like-finite temperature fluctuation, and squeezing process. $\chi(t)$ denotes a coherence process formed by the driving field and non-Markovian environment.

In Heisenberg picture, operators change with the time, but quantum states are time-independent. Therefore, with given $\rho_{SR}(0)$ given by Eq. (24), the time evolution of any physical observable can be obtained directly from Eq. (4) through the identity

$$\mathrm{Tr}_{SR}[\hat{P}(t)\rho_{SR}(0)] \equiv \mathrm{Tr}_S[\hat{P}(t)\rho_S(t)], \tag{27}$$

in which $\hat{P}(t)$ is polynomial of the cavity field operators $\hat{a}(t)$ and $\hat{a}^\dagger(t)$, i.e., $\hat{P}(t) \equiv \hat{P}(\hat{a}(t), \hat{a}^\dagger(t)) = \sum_{N_1,N_2=0}^{\infty} \hat{a}(t)^{\dagger N_1}\hat{a}(t)^{N_2} \equiv \sum_{N_1,N_2=0}^{\infty} \hat{P}_{N_1N_2}(t)$. In this case, the cavity state $\rho(t) = \mathrm{Tr}_R\rho_{SR}(t)$ with $\rho_{SR}(t) = U(t)\rho_{SR}(0)U^\dagger(t)$ which describes the density matrix of the total system, and $\mathrm{Tr}_{SR} \equiv \mathrm{Tr}_S\mathrm{Tr}_R$ denotes traces over the system and environment, respectively. $\rho_{SR}(0)$ is the total initial state given by Eq. (24). With the identity Eq. (27) and use of Eq. (4), we can obtain these coefficients as follows:

$$\begin{aligned}\mathcal{S}(t) =& -\beta(t)/2i, \\ \mathcal{E}(t) =& -\mathrm{Im}[\alpha(t)], \\ \chi(t) =& i[\dot{\mu}(t) - \alpha(t)\mu(t) - \beta(t)\mu^*(t)], \\ \gamma_1(t) =& -0.5\dot{\mathcal{V}}(t)/\mathcal{V}(t), \\ \gamma_2(t) =& [\partial/\partial t + 2\Gamma_1(t)]\langle\hat{\sigma}^\dagger\hat{\sigma}\rangle - \{\beta^*(t)\langle\hat{\sigma}^2\rangle + \mathrm{H.c.}\}, \\ \gamma_3(t) =& (\alpha(t) - 0.5\partial/\partial t)\langle\hat{\sigma}^2\rangle + \frac{\beta(t)}{2}\langle\hat{\sigma}\hat{\sigma}^\dagger + \hat{\sigma}^\dagger\hat{\sigma}\rangle, \end{aligned} \tag{28}$$

where $\alpha(t)$, $\beta(t)$, and $\mathcal{V}(t)$ are given by

$$\begin{aligned}\alpha(t) =& (\dot{\mathcal{X}}\mathcal{X}^* - \dot{\mathcal{Y}}\mathcal{Y}^*)/\mathcal{V}(t), \\ \beta(t) =& (\mathcal{X}\dot{\mathcal{Y}} - \dot{\mathcal{X}}\mathcal{Y})/\mathcal{V}(t), \\ \mathcal{V}(t) =& |\mathcal{X}(t)|^2 - |\mathcal{Y}(t)|^2, \end{aligned} \tag{29}$$

where $\mathcal{X}(t)$ and $\mathcal{Y}(t)$ are given by Eq. (7).

In this section, we discuss the effects of the non-Markovian environment on nonreciprocal single-photon blockade with Gaussian Ornstein-Uhlenbeck process given by Eq. (10) (In numerical simulations, we do not consider $\gamma_2(t)$ because it is much smaller than $\gamma_1(t)$ and $\gamma_3(t)$ under given parameters [82]). In Fig. 4 with driving the device from the left side, we show the second-order correlation function $g^{(2)}(0)$ as a function of the driving strength f with the different spectral width of environment λ by numerically solving master Eq. (25). The figure is plotted in the weak driving limit. We notice that *the nonreciprocal unconventional single-photon blockade* occurs in Fig. 4 due to the quantum interference between two different pathways shown in Fig. 1(c), which are produced by the OPA pump and driving field, respectively. When we add laser driving the device from the right side, the occurrence of the photon bunching can be found in Fig. 4.

To be specific, for a given spectral width of environment, e.g., increasing from $\lambda = 2.1\gamma \sim 10\gamma$, we find from the figure that the optimal point f_{opt} decreases from $f = 0.036\gamma$, $f = 0.035\gamma$, $f = 0.034\gamma$, to $f = 0.033\gamma$. As the spectrum width of the environment is further increased, $\lambda = 300\gamma$, the optimal value f is given by Eq. (18) (in this case, optimal value $f = 0.03\gamma$), where the driving phase takes the optimal values $\phi = \phi_{\mathrm{opt}}$ given by Eq. (19). For the sake of clarity, we separately draw the non-Markovin case and the Markovian limit case when the environmental spectrum width $\lambda = 300\gamma$ in Fig. 5. This figure shows the consistency of nonreciprocal unconventional single-photon blockade between non-Markovian limit with $\lambda = 300\gamma$ and Markovian approximation.

VI. DISCUSSIONS ON THE EXPERIMENTAL IMPLEMENTATION

In this section, we present a discussion on the experimental feasibility to observe the prediction in an optical cavity. For the model under study, we mainly focus on the following two points: (i) Fizeau shift, (ii) two-photon driving.

(i) The experimental feasible parameters are as follows [142–146]: $\lambda = 1550$ nm, $r = 30\mu$m, $\Omega \sim 3 \times 10^9$ Hz, $n = 1.4$, $Q = 1.5 \times 10^5$. With these parameters, we have the Sagnac-Fizeau shift $|\Delta_F/2\pi| \sim 42491.6$ MHz and decay of cavity $\gamma/2\pi \sim 8109.11$ MHz, which leads to $|\Delta_F/\gamma| \sim 5.24$. In our work, $|\Delta_F/\gamma| = 5$ (see the caption of Fig. 2) is within touch of current experimental technology.

In addition, Fig. 6 shows the ratio of Fizeau drag [$\Delta_F = \pm\frac{nr\Omega\omega}{c}(1 - \frac{1}{n^2} - \frac{\lambda}{n}\frac{dn}{d\lambda}) \equiv \beta\Omega$] to decay rate as the angular velocity of the cavity increases [also see Fig. 4, where $|\Delta_F| = 0.004\gamma$)], where spinning cavities have reached much higher velocities, for example, the GHz regimes [147,148].

(ii) The two-photon driving term can be realized by a degenerate optical parametric amplifier (OPA) in a single cavity containing a $\chi^{(2)}$ nonlinear medium. In this case, the OPA system can be described by Hamiltonian

$$\begin{aligned}\tilde{H}_{OPA} =& \omega_c\hat{a}^\dagger\hat{a} + \omega_p\hat{p}^\dagger\hat{p} + J_p(\hat{a}^{\dagger 2}\hat{p} + \hat{p}^\dagger\hat{a}^2) \\ &+ F(t)\hat{a}^\dagger + F^*(t)\hat{a}, \end{aligned} \tag{30}$$

where $\hat{a}$ and $\hat{p}$ are the photon annihilation operators of the two cavity modes with frequencies ω_c and ω_p, respectively. $F(t)$ is the single-photon driving strength. J_p denotes the coupling

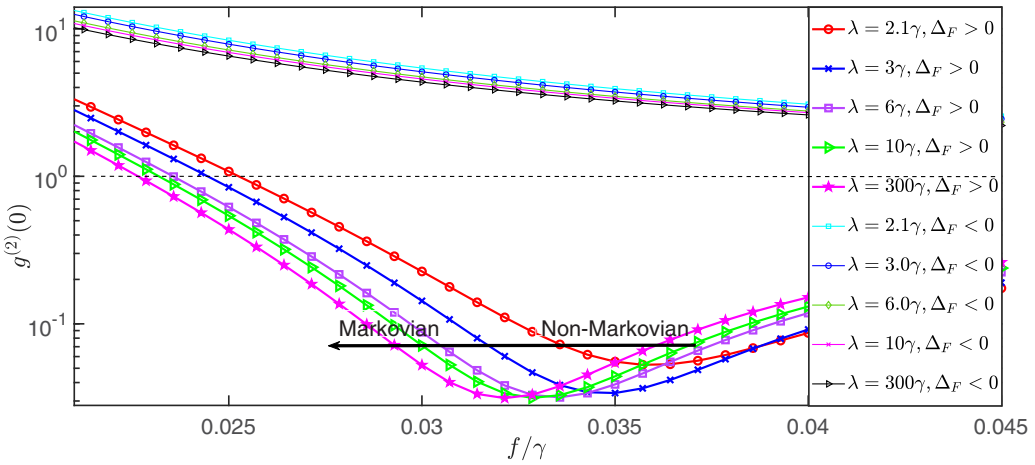

FIG. 4. The second-order correlation function $g^{(2)}(0)$ varies with the driving strength f for different input directions. For the driving on the cavity from the left side, $\Delta_F > 0$, the figure shows the influence of the non-Markovian environment on the nonreciprocal unconventional photon blockade with the second-order correlation function $g^{(2)}(0)$ by numerically solving master Eq. (13) as a function of the driving strength f in unconventional single-photon blockade regime. ϕ takes its optimal value ϕ_{opt} given by Eq. (19). From the figure, we point out that as the increase of the environmental spectrum width λ, the non-Markovian unconventional single-photon blockade effect gradually tends to the case of Markovian limit ($\lambda \to \infty$ or $\lambda \gg \gamma$). In contrast, for the driving on the cavity from the right side, $\Delta_F < 0$, the photon bunching occurs. Parameters chosen are $g = 0.002\gamma$, $\Delta_l = 0$, $|\Delta_F| = 0.004\gamma$, $\theta = 4$rad. The chosen parameters satisfy $(\Delta_F + \Delta_l)^2 = 4g^4$, which leads to the time-dependent coefficients of Eq. (25) to have analytical steady solutions.

strength via $\chi^{(2)}$ nonlinear medium [149], which mediates the conversion of a photon in cavity p to two photons in cavity a [12,48,49]. The coupling strength between two cavities is given by

$$J_p = D\varepsilon_0\left(\frac{\hbar\omega_c}{2\varepsilon_0}\right)\sqrt{\frac{\hbar\omega_p}{2\varepsilon_0}}\int d\mathbf{r}\frac{\chi^{(2)}(\mathbf{r})}{[\varepsilon(\mathbf{r})]^3}\alpha_1^2(\mathbf{r})\alpha_2(\mathbf{r}), \quad (31)$$

where ε_0 is the vacuum permittivity. $\varepsilon(\mathbf{r})$ denotes the relative permittivity. D is a degeneracy factor. $\alpha_1(\mathbf{r})$ and $\alpha_2(\mathbf{r})$ are the wave functions for mode $\hat{a}_1$ and mode $\hat{a}_2$, respectively.

It is widely recognized that all quantum amplifiers are essentially nonlinear system [113,149]. As one of the examples of parametric amplification nonlinear interactions, the schematic diagram of the OPA physical process is shown in Fig. 7. The OPA interaction involves a pump photon with frequency ω_p being converted into two photons with identical frequency ω_c with the relation $\omega_p = 2\omega_c$ due to the second-order nonlinearity. The pump field is treated approximately as a classical coherent field because the pump field depletion is negligible [150–152], namely, $\hat{p} \to \beta e^{-i(\theta_p - \omega_p t)}$ (mean-field approximation, which requires pump field amplitude very large), with β and θ_p being the amplitude and the phase of

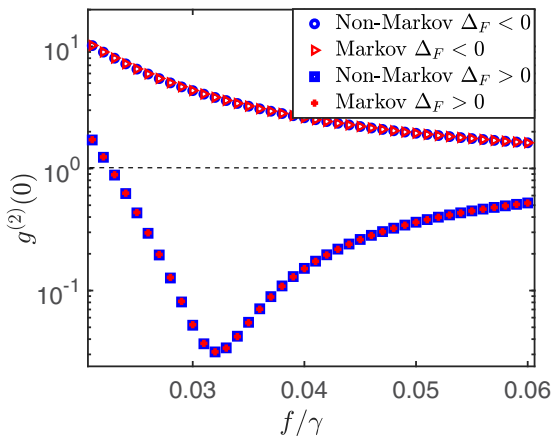

FIG. 5. The second-order correlation function $g^{(2)}(0)$ varies with the driving strength f for different input directions. This figure shows the consistency of nonreciprocal unconventional single-photon blockade between non-Markovian limit with $\lambda = 300\gamma$ given by Eq. (25) and Markovian approximation given by Eq. (13). The parameters chosen are the same as those in Fig. 4.

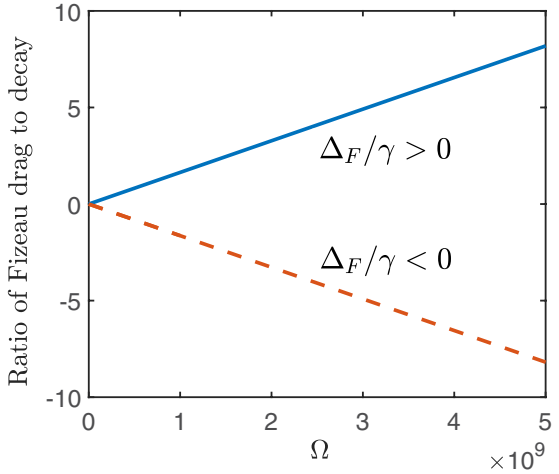

FIG. 6. Ratio Δ_F/γ of Fizeau drag to decay versus angular velocity (The unit of Ω is Hz) of the cavity for $\Delta_F/\gamma > 0$ (blue line) and $\Delta_F/\gamma < 0$ (red-dashed line) cases. The optical wavelength is $\lambda = 1.5$ μm, the radius of the cavity is $r = 30$ μm, and the linear refractive index of the cavity is $n = 1.4$.

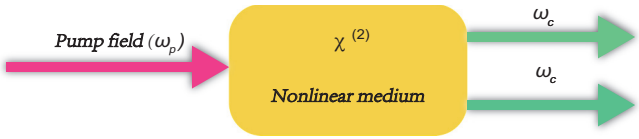

FIG. 7. Our model consists of spinning cavity coupled with a degenerate optical parametric amplifier (OPA) [12,58,81,83,113–120] and single-photon laser driving. The figure represents the OPA process: A pump photon with frequency ω_p is down-converted into an identical pair of photons with frequency ω_c after passing through the $\chi^{(2)}$ nonlinear medium.

the pump field. In this case with a rotating frame, the OPA Hamiltonian Eq. (30) becomes

$$\hat{H}_{\rm OPA} = \Delta_l \hat{a}^\dagger \hat{a} + G\hat{a}^{\dagger 2} + G^* \hat{a}^2 + F\hat{a}^\dagger + F^* \hat{a}, \qquad (32)$$

where $\Delta_l = \omega_c - \omega_l$, and $G = J_p \beta e^{-i\theta_p} \equiv g e^{-i\theta}$ is the nonlinear gain of the OPA with J_p given by Eq. (31). Obviously, G is directly proportional to the amplitude of the pump field and the second-order nonlinearity of the medium.

It is worth evaluating the actual experimental possibility of the strong photon antibunching effect with weak nonlinearity. To estimate the coupling strength between the modes, we simplify the expression in Eq. (31) as

$$g = \beta \tilde{\chi}^{(2)} \left(\frac{\omega_c}{\varepsilon_r}\right)^{3/2} \sqrt{\frac{\hbar}{\varepsilon_0 V_{\rm eff}}}, \qquad (33)$$

where $D = 2$ and $\alpha_1(\mathbf{r}) = \alpha_2(\mathbf{r}) = \alpha(\mathbf{r})$. In this situation, an effective mode volume for the scalar field profile is defined in Eq. (33) as $V_{\rm eff}^{-1/2} = \int [\alpha(\mathbf{r})]^3 d^3\mathbf{r}$. Furthermore, we assume the real part of $\chi^{(2)}$ constant denoted by $\tilde{\chi}^{(2)}$. Taking a simple normalized mode profile $\alpha(\mathbf{r}) = (2/\pi\sigma_x\sigma_y d)^{1/2} \exp(-x^2/2\sigma_x^2 - y^2/2\sigma_y^2) \cos(\pi/d)z$ for photonic crystal resonators at near infrared wavelengths [153], we analytically gets $V_{\rm eff} = a\pi\sigma_x\sigma_y d/3$.

In dielectric photonic microcavities [154], we may take $\sigma_x = \lambda/(2\sqrt{\varepsilon_r})$, $\sigma_y = d = \sigma_x/3$, $\varepsilon_r = 2$, and $\beta = 100$. With these values, and assuming $\lambda = 1.5\ \mu$m, the mode volume estimated from the expression above is $V_{\rm eff} \simeq 0.07\ \mu{\rm m}^3$. The present scheme could be realized with state-of-art technology employing the main III–V materials, such as GaAs [119,155], where bulk nonlinear susceptibility can be of the order of 10–200 pm/V in optoelectronics. Taking these values into account, we get a realistic order of magnitude estimate for the coupling constant in Eq. (31) as $\hbar g \sim 0.018\ \mu$eV, which is a remarkably large value for a passive nonlinear material. In standard III–V semiconductor microresonators with quality factors on the order of 10^5, therefore, $Q = 1.5 \times 10^5$ [156] is reasonable, which leads to $\hbar\gamma \sim 2.76\ \mu$eV. The two-photon driving strength is $g/\gamma \sim 0.0065$ (we take $g/\gamma \sim 0.0045$ in our simulations [12,83,113–120], see Fig. 2). Hence, the proposal could be realizable within touch of current technologies.

VII. CONCLUSIONS AND DISCUSSIONS

In summary, we have studied the nonreciprocal unconventional photon blockade in a system consisting of spinning cavity coupled respectively with degenerate optical parametric amplifier (OPA) and the laser driving with weak nonlinearities through the Fizeau drag. Due to the destructive quantum interference effect between the different paths for two-photon space, strong antibunching effects have been found when driving on the cavity from the left side. While driving on the cavity from the right side, the quantum interference paths are broken, which leads to the occurrence of the photon bunching. By analytical calculations, we derive a condition for optimized photon antibunching. With these parameters, the value of the equal-time second-order correlation function gets minimum, which corresponds to single-photon blockade. We find that the analytical expressions of the equal-time second-order correlation function are in good agreement with those obtained by the fully numerical simulation by numerically solving the master equation. Moreover, we extend the above results to the non-Markovian bath which consists of collection of infinite oscillators (bosonic photonic modes). We show nonreciprocal unconventional photon blockades exhibit a transition from the non-Markovian to Markovian regime by controlling environmental spectral width regardless of the weakness of OPA gain and driving field.

Applications of nonreciprocal unconventional photon blockade to a variety of physically relevant systems as well as its extension to wide class of open quantum system with spinning cavities through the Fizeau drag, e.g., (1) $\chi^{(2)}$ nonlinear materials $J(\hat{a}^2\hat{b}^\dagger + \hat{b}\hat{a}^{\dagger 2})$, (2) Kerr nonlinear mediums $U\hat{a}^{\dagger 2}\hat{a}^2$, (3) Jaynes-Cummings models $\sum_k g_k(\sigma_- b_k^\dagger + b_k\sigma_+)$ [67,157–161], or Rabi models $\sum_k v_k\sigma_x(b_k^\dagger + b_k)$ [162,163], (4) optomechanical systems $\hat{a}^\dagger\hat{a}(\hat{b}+\hat{b}^\dagger)$ [164–166], coupled with the non-Markovian baths, deserve future investigations.

ACKNOWLEDGMENTS

This work is supported by National Natural Science Foundation of China (NSFC) under Grants No. 11534002 and No. 11705025, Fundamental Research Funds for the Central Universities under Grant No. 2412019FZ044, and Science Foundation of the Education Department of Jilin Province during the 13th Five Year Plan Period under Grant No. JJKH20190262KJ.

[1] V. Giovannetti, S. Lloyd, and L. Maccone, Advances in quantum metrology, Nat. Photon. **5**, 222 (2011).
[2] E. Knill, R. Laflamme, and G. J. Milburn, A scheme for efficient quantum computation with linear optics, Nature (London) **409**, 46 (2001).
[3] P. Kok, W. J. Munro, K. Nemoto, T. C. Ralph, J. P. Dowling, and G. J. Milburn, Linear optical quantum computing with photonic qubits, Rev. Mod. Phys. **79**, 135 (2007).
[4] A. Imamoğlu, H. Schmidt, G. Woods, and M. Deutsch, Strongly Interacting Photons in a Nonlinear Cavity, Phys. Rev. Lett. **79**, 1467 (1997).
[5] K. M. Birnbaum, A. Boca, R. Miller, A. D. Boozer, T. E. Northup, and H. J. Kimble, Photon blockade in an optical cavity with one trapped atom, Nature (London) **436**, 87 (2005).
[6] A. Faraon, I. Fushman, D. Englund, N. Stoltz, P. Petroff, and J. Vučković, Coherent generation of nonclassical light on a chip

via photon-induced tunneling and blockade, Nat. Phys. **4**, 859 (2008).

[7] L. Tian and H. J. Carmichael, Quantum trajectory simulations of two-state behavior in an optical cavity containing one atom, Phys. Rev. A **46**, R6801(R) (1992).

[8] M. J. Werner and A. Imamoğlu, Photon-photon interactions in cavity electromagnetically induced transparency, Phys. Rev. A **61**, 011801(R) (1999).

[9] R. J. Brecha, P. R. Rice, and M. Xiao, N two-level atoms in a driven optical cavity: Quantum dynamics of forward photon scattering for weak incident fields, Phys. Rev. A **59**, 2392 (1999).

[10] S. Rebić, S. M. Tan, A. S. Parkins, and D. F. Walls, Large Kerr nonlinearity with a single atom, J. Opt. B **1**, 490 (1999).

[11] X. Y. Liang, Z. L. Duan, Q. Guo, C. J. Liu, S. G. Guan, and Y. Ren, Antibunching effect of photons in a two-level emitter-cavity system, Phys. Rev. A **100**, 063834 (2019).

[12] Y. Y. Yan, Y. B. Cheng, S. G. Guan, D. Y. Yu, and Z. L. Duan, Pulse-regulated single-photon generation via quantum interference in a $\chi^{(2)}$ nonlinear nanocavity, Opt. Lett. **43**, 5086 (2018).

[13] J. M. Fink, A. Dombi, A. Vukics, A. Wallraff, and P. Domokos, Observation of the Photon-Blockade Breakdown Phase Transition, Phys. Rev. X **7**, 011012 (2017).

[14] C. Hamsen, K. N. Tolazzi, T. Wilk, and G. Rempe, Two-Photon Blockade in an Atom-Driven Cavity QED System, Phys. Rev. Lett. **118**, 133604 (2017).

[15] C. L. Zhai, R. Huang, B. J. Li, H. Jing, and L. M. Kuang, Mechanical engineering of photon blockades in a cavity optomechanical system, arXiv:1901.07654.

[16] K. Hou, C. J. Zhu, Y. P. Yang, and G. S. Agarwal, Interfering pathways for photon blockade in cavity QED with one and two qubits, Phys. Rev. A **100**, 063817 (2019).

[17] A. Miranowicz, M. Paprzycka, Y. X. Liu, J. Bajer, and F. Nori, Two-photon and three-photon blockades in driven nonlinear systems, Phys. Rev. A **87**, 023809 (2013).

[18] M. Leib, F. Deppe, A. Marx, R. Gross, and M. J. Hartmann, Networks of nonlinear superconducting transmission line resonators, New J. Phys. **14**, 075024 (2012).

[19] M. Leib and M. J. Hartmann, Bose-Hubbard dynamics of polaritons in a chain of circuit quantum electrodynamics cavities, New J. Phys. **12**, 093031 (2010).

[20] C. J. Zhu, Y. P. Yang, and G. S. Agarwal, Collective multiphoton blockade in cavity quantum electrodynamics, Phys. Rev. A **95**, 063842 (2017).

[21] J. Z. Lin, K. Hou, C. J. Zhu, and Y. P. Yang, Manipulation and improvement of multiphoton blockade in a cavity-QED system with two cascade three-level atoms, Phys. Rev. A **99**, 053850 (2019).

[22] J. Kim, O. Bensen, H. Kan, and Y. Yamamoto, A single-photon turnstile device, Nature **397**, 500 (1999); I. I. Smolyaninov, A. V. Zayats, A. Gungor, and C. C. Davis, Single-Photon Tunneling via Localized Surface Plasmons, Phys. Rev. Lett. **88**, 187402 (2002); S. Rebić, A. S. Parkins, and S. M. Tan, Photon statistics of a single-atom intracavity system involving electromagnetically induced transparency, Phys. Rev. A **65**, 063804 (2002); D. G. Angelakis, M. F. Santos, and S. Bose, Photon-blockade-induced Mott transitions and XY spin models in coupled cavity arrays, *ibid.* **76**, 031805(R) (2007); Y. X. Liu, X.-W. Xu, A. Miranowicz, and F. Nori, From blockade to transparency: Controllable photon transmission through a circuit-QED system, *ibid.* **89**, 043818 (2014); A. Faraon, A. Majumdar, and J. Vučković, Generation of nonclassical states of light via photon blockade in optical nanocavities, *ibid.* **81**, 033838 (2010).

[23] A. J. Hoffman, S. J. Srinivasan, S. Schmidt, L. Spietz, J. Aumentado, H. E. Türeci, and A. A. Houck, Dispersive Photon Blockade in a Superconducting Circuit, Phys. Rev. Lett. **107**, 053602 (2011).

[24] C. Lang, D. Bozyigit, C. Eichler, L. Steffen, J. M. Fink, A. A. Abdumalikov, Jr., M. Baur, S. Filipp, M. P. da Silva, A. Blais, and A. Wallraff, Observation of Resonant Photon Blockade at Microwave Frequencies using Correlation Function Measurements, Phys. Rev. Lett. **106**, 243601 (2011).

[25] P. Rabl, Photon Blockade Effect in Optomechanical Systems, Phys. Rev. Lett. **107**, 063601 (2011).

[26] A. Nunnenkamp, K. Børkje, and S. M. Girvin, Single-Photon Optomechanics, Phys. Rev. Lett. **107**, 063602 (2011).

[27] J.-Q. Liao and C. K. Law, Correlated two-photon transport in a one-dimensional waveguide side-coupled to a nonlinear cavity, Phys. Rev. A **82**, 053836 (2010).

[28] J.-Q. Liao and F. Nori, Photon blockade in quadratically coupled optomechanical systems, Phys. Rev. A **88**, 023853 (2013).

[29] X. Y. Lü, Y. Wu, J. R. Johansson, H. Jing, J. Zhang, and F. Nori, Squeezed Optomechanics with Phase-Matched Amplification and Dissipation, Phys. Rev. Lett. **114**, 093602 (2015).

[30] P. Kómár, S. D. Bennett, K. Stannigel, S. J. M. Habraken, P. Rabl, P. Zoller, and M. D. Lukin, Single-photon nonlinearities in two-mode optomechanics, Phys. Rev. A **87**, 013839 (2013).

[31] X. Y. Lü, W. M. Zhang, S. Ashhab, Y. Wu, and F. Nori, Quantum-criticality-induced strong Kerr nonlinearities in optomechanical systems, Sci. Rep. **3**, 2943 (2013).

[32] X. N. Xu, M. Gullans, and J. M. Taylor, Quantum nonlinear optics near optomechanical instabilities, Phys. Rev. A **91**, 013818 (2015).

[33] A. Miranowicz, J. Bajer, N. Lambert, Y. X. Liu, and F. Nori, Tunable multiphonon blockade in coupled nanomechanical resonators, Phys. Rev. A **93**, 013808 (2016).

[34] H. Xie, G. W. Lin, X. Chen, Z. H. Chen, and X. M. Lin, Single-photon nonlinearities in a strongly driven optomechanical system with quadratic coupling, Phys. Rev. A **93**, 063860 (2016).

[35] H. Xie, C. G. Liao, X. Shang, M. Y. Ye, and X. M. Lin, Phonon blockade in a quadratically coupled optomechanical system, Phys. Rev. A **96**, 013861 (2017).

[36] H. Wang, X. Gu, Y. X. Liu, A. Miranowicz, and F. Nori, Tunable photon blockade in a hybrid system consisting of an optomechanical device coupled to a two-level system, Phys. Rev. A **92**, 033806 (2015).

[37] F. Zou, L. B. Fan, J. F. Huang, and J.-Q. Liao, Enhancement of few-photon optomechanical effects with cross-Kerr nonlinearity, Phys. Rev. A **99**, 043837 (2019).

[38] Y. X. Liu, A. Miranowicz, Y. B. Gao, J. Bajer, C. P. Sun, and F. Nori, Qubit-induced phonon blockade as a signature of quantum behavior in nanomechanical resonators, Phys. Rev. A **82**, 032101 (2010).

[39] Y. Qu, J. H. Li, and Y. Wu, Interference-modulated photon statistics in whispering-gallery-mode microresonator optomechanics, Phys. Rev. A **99**, 043823 (2019).

[40] J. C. López Carreño, C. Sánchez Muñoz, D. Sanvitto, E. del Valle, and F. P. Laussy, Exciting Polaritons with Quantum Light, Phys. Rev. Lett. **115**, 196402 (2015).

[41] T. Grujic, S. R. Clark, D. Jaksch, and D. G. Angelakis, Non-equilibrium many-body effects in driven nonlinear resonator arrays, New J. Phys. **14**, 103025 (2012).

[42] A. L. Boité, M. J. Hwang, H. Nha, and M. B. Plenio, Fate of photon blockade in the deep strong-coupling regime, Phys. Rev. A **94**, 033827 (2016).

[43] A. Ridolfo, M. Leib, S. Savasta, and M. J. Hartmann, Photon Blockade in the Ultrastrong Coupling Regime, Phys. Rev. Lett. **109**, 193602 (2012).

[44] M. Radulaski, K. A. Fischer, K. G. Lagoudakis, J. L. Zhang, and J. Vučković, Photon blockade in two-emitter-cavity systems, Phys. Rev. A **96**, 011801(R) (2017).

[45] S. Ghosh and T. C. H. Liew, Dynamical Blockade in a Single-Mode Bosonic System, Phys. Rev. Lett. **123**, 013602 (2019).

[46] A. P. Foster, D. Hallett, I. V. Iorsh, S. J. Sheldon, M. R. Godsland, B. Royall, E. Clarke, I. A. Shelykh, A. M. Fox, M. S. Skolnick, I. E. Itskevich, and L. R. Wilson, Tunable Photon Statistics Exploiting the Fano Effect in a Waveguide, Phys. Rev. Lett. **122**, 173603 (2019).

[47] M. Bajcsy, A. Majumdar, A. Rundquist, and J. Vučković, Photon blockade with a four-level quantum emitter coupled to a photonic-crystal nanocavity, New J. Phys. **15**, 025014 (2013).

[48] A. Majumdar and D. Gerace, Single-photon blockade in doubly resonant nanocavities with second-order nonlinearity, Phys. Rev. B **87**, 235319 (2013).

[49] H. Z. Shen, Y. H. Zhou, and X. X. Yi, Quantum optical diode with semiconductor microcavities, Phys. Rev. A **90**, 023849 (2014).

[50] T. E. Lee and M. C. Cross, Quantum-classical transition of correlations of two coupled cavities, Phys. Rev. A **88**, 013834 (2013).

[51] D. Gerace, H. E. Türeci, A. Imamoglu, V. Giovannetti, and R. Fazio, The quantum-optical Josephson interferometer, Nat. Phys. **5**, 281 (2009).

[52] F. Fratini, E. Mascarenhas, L. Safari, J-Ph. Poizat, D. Valente, A. Auffèves, D. Gerace, and M. F. Santos, Fabry-Perot Interferometer with Quantum Mirrors: Nonlinear Light Transport and Rectification, Phys. Rev. Lett. **113**, 243601 (2014).

[53] E. Mascarenhas, D. Gerace, D. Valente, S. Montangero, A. Auffèves, and M. F. Santos, A quantum optical valve in a nonlinear-linear resonators junction, Europhys. Lett. **106**, 54003 (2014).

[54] D. E. Chang, A. S. Sørensen, E. A. Demler, and M. D. Lukin, A single-photon transistor using nanoscale surface plasmons, Nat. Phys. **3**, 807 (2007).

[55] T. C. H. Liew and V. Savona, Single Photons from Coupled Quantum Modes, Phys. Rev. Lett. **104**, 183601 (2010).

[56] H. J. Carmichael, Photon Antibunching and Squeezing for a Single Atom in a Resonant Cavity, Phys. Rev. Lett. **55**, 2790 (1985).

[57] M. Bamba, A. Imamoğlu, I. Carusotto, and C. Ciuti, Origin of strong photon antibunching in weakly nonlinear photonic molecules, Phys. Rev. A **83**, 021802(R) (2011).

[58] H. Flayac and V. Savona, Unconventional photon blockade, Phys. Rev. A **96**, 053810 (2017).

[59] E. Z. Casalengua, J. C. L. Carreño, F. P. Laussy, and E. del Valle, Conventional and unconventional photon statistics, arXiv:1901.09030.

[60] C. Vaneph, A. Morvan, G. Aiello, M. Féchant, M. Aprili, J. Gabelli, and J. Estève, Observation of the Unconventional Photon Blockade in the Microwave Domain, Phys. Rev. Lett. **121**, 043602 (2018).

[61] H. J. Snijders, J. A. Frey, J. Norman, H. Flayac, V. Savona, A. C. Gossard, J. E. Bowers, M. P. van Exter, D. Bouwmeester, and W. Löffler, Observation of the Unconventional Photon Blockade, Phys. Rev. Lett. **121**, 043601 (2018).

[62] X.-W. Xu and Y. Li, Tunable photon statistics in weakly nonlinear photonic molecules, Phys. Rev. A **90**, 043822 (2014).

[63] I. Carusotto and C. Ciuti, Quantum fluids of light, Rev. Mod. Phys. **85**, 299 (2013); X.-W. Xu and Y. Li, Strongly correlated two-photon transport in a one-dimensional waveguide coupled to a weakly nonlinear cavity, Phys. Rev. A **90**, 033832 (2014); J. T. Shen and S. H. Fan, Strongly Correlated Two-Photon Transport in a One-Dimensional Waveguide Coupled to a Two-Level System, Phys. Rev. Lett. **98**, 153003 (2007); X.-W. Xu and Y. Li, Strong photon antibunching of symmetric and antisymmetric modes in weakly nonlinear photonic molecules, Phys. Rev. A **90**, 033809 (2014); T. C. H. Liew and V. Savona, Multimode entanglement in coupled cavity arrays, New J. Phys. **15**, 025015 (2013).

[64] M. Bamba and C. Ciuti, Counter-polarized single-photon generation from the auxiliary cavity of a weakly nonlinear photonic molecule, Appl. Phys. Lett. **99**, 171111 (2011); O. Kyriienko, I. A. Shelykh, and T. C. H. Liew, Tunable single-photon emission from dipolaritons, Phys. Rev. A **90**, 033807 (2014); T. C. H. Liew and V. Savona, Quantum entanglement in nanocavity arrays, *ibid.* **85**, 050301(R) (2012).

[65] A. Majumdar, M. Bajcsy, A. Rundquist, and J. Vučković, Loss-Enabled Sub-Poissonian Light Generation in a Bimodal Nanocavity, Phys. Rev. Lett. **108**, 183601 (2012).

[66] W. Zhang, Z. Y. Yu, Y. M. Liu, and Y. W. Peng, Optimal photon antibunching in a quantum-dot-bimodal-cavity system, Phys. Rev. A **89**, 043832 (2014).

[67] J. Tang, W. D. Geng, and X. L. Xu, Quantum interference induced photon blockade in a coupled single quantum dot-cavity system, Sci. Rep. **5**, 9252 (2015).

[68] H. Flayac and V. Savona, Single photons from dissipation in coupled cavities, Phys. Rev. A **94**, 013815 (2016).

[69] H. Z. Shen, Y. H. Zhou, and X. X. Yi, Tunable photon blockade in coupled semiconductor cavities, Phys. Rev. A **91**, 063808 (2015).

[70] H. Flayac, D. Gerace, and V. Savona, An all-silicon single-photon source by unconventional photon blockade, Sci. Rep. **5**, 11223 (2015).

[71] H. Z. Shen, Y. H. Zhou, H. D. Liu, G. C. Wang, and X. X. Yi, Exact optimal control of photon blockade with weakly nonlinear coupled cavities, Opt. Exp. **23**, 32835 (2015).

[72] Y. H. Zhou, H. Z. Shen, and X. X. Yi, Unconventional photon blockade with second-order nonlinearity, Phys. Rev. A **92**, 023838 (2015).

[73] H. Z. Shen, S. Xu, Y. H. Zhou, G. C. Wang, and X. X. Yi, Unconventional photon blockade from bimodal driving and dissipations in coupled semiconductor microcavities, J. Phys. B **51**, 035503 (2018).

[74] Y. H. Zhou, H. Z. Shen, X. Q. Shao, and X. X. Yi, Strong photon antibunching with weak second-order nonlinearity under dissipation and coherent driving, Opt. Express **24**, 17332 (2016).

[75] H. Flayac and V. Savona, Input-output theory of the unconventional photon blockade, Phys. Rev. A **88**, 033836 (2013); D. Gerace and V. Savona, Unconventional photon blockade in doubly resonant microcavities with second-order nonlinearity, *ibid.* **89**, 031803(R) (2014); S. Ferretti, V. Savona, and D. Gerace, Optimal antibunching in passive photonic devices based on coupled nonlinear resonators, New J. Phys. **15**, 025012 (2013).

[76] F. Zou, D.-G. Lai, and J.-Q. Liao, Photon blockade effect in a coupled cavity system, arXiv:1803.06642; O. Kyriienko and T. C. H. Liew, Triggered single-photon emitters based on stimulated parametric scattering in weakly nonlinear systems, Phys. Rev. A **90**, 063805 (2014).

[77] X.-W. Xu and Y. J. Li, Antibunching photons in a cavity coupled to an optomechanical system, J. Opt. B: At. Mol. Opt. Phys. **46**, 035502 (2013).

[78] V. Savona, Unconventional photon blockade in coupled optomechanical systems, arXiv:1302.5937.

[79] S. Dufferwiel, F. Fras, A. Trichet, P. M. Walker, F. Li, L. Giriunas, M. N. Makhonin, L. R. Wilson, J. M. Smith, E. Clarke, M. S. Skolnick, and D. N. Krizhanovskii, Strong exciton-photon coupling in open semiconductor microcavities, Appl. Phys. Lett. **104**, 192107 (2014).

[80] Y. H. Zhou, H. Z. Shen, X. Y. Zhang, and X. X. Yi, Zero eigenvalues of a photon blockade induced by a non-Hermitian Hamiltonian with a gain cavity, Phys. Rev. A **97**, 043819 (2018).

[81] M. A. Lemonde, N. Didier, and A. A. Clerk, Antibunching and unconventional photon blockade with Gaussian squeezed states, Phys. Rev. A **90**, 063824 (2014).

[82] H. Z. Shen, C. Shang, Y. H. Zhou, and X. X. Yi, Unconventional single-photon blockade in non-Markovian systems, Phys. Rev. A **98**, 023856 (2018).

[83] B. Sarma and A. K. Sarma, Quantum-interference-assisted photon blockade in a cavity via parametric interactions, Phys. Rev. A **96**, 053827 (2017).

[84] D. Jalas, A. Petrov, M. Eich, W. Freude, S. H. Fan, Z. F. Yu, R. Baets, M. Popović, A. Melloni, J. D. Joannopoulos, M. Vanwolleghem, C. R. Doerr, and H. Renner, What is- and what is not-an optical isolator, Nat. Photon. **7**, 579 (2013).

[85] D. L. Sounas and A. Alù, Non-reciprocal photonics based on time modulation, Nat. Photon. **11**, 774 (2017).

[86] C. Sayrin, C. Junge, R. Mitsch, B. Albrecht, D. O'Shea, P. Schneeweiss, J. Volz, and A. Rauschenbeutel, Nanophotonic Optical Isolator Controlled by the Internal State of Cold Atoms, Phys. Rev. X **5**, 041036 (2015).

[87] L. Tang, J. S. Tang, W. D. Zhang, G. W. Lu, H. Zhang, Y. Zhang, K. Y. Xia, and M. Xiao, On-chip chiral single-photon interface: Isolation and unidirectional emission, Phys. Rev. A **99**, 043833 (2019).

[88] M. Scheucher, A. Hilico, E. Will, J. Volz, and A. Rauschenbeutel, Quantum optical circulator controlled by a single chirally coupled atom, Science **354**, 1577 (2016).

[89] X.-W. Xu, Y.-J. Zhao, H. Wang, H. Jing, and A.-X. Chen, Nonreciprocal photon blockade via quadratic optomechanical coupling, arXiv:1809.07596.

[90] S. Manipatruni, J. T. Robinson, and M. Lipson, Optical Nonreciprocity in Optomechanical Structures, Phys. Rev. Lett. **102**, 213903 (2009).

[91] Z. Shen, Y. L. Zhang, Y. Chen, C. L. Zou, Y. F. Xiao, X. B. Zou, F. W. Sun, G. C. Guo, and C. H. Dong, Experimental realization of optomechanically induced non-reciprocity, Nat. Photonics **10**, 657 (2016).

[92] N. R. Bernier, L. D. Tóth, A. Koottandavida, M. A. Ioannou, D. Malz, A. Nunnenkamp, A. K. Feofanov, and T. J. Kippenberg, Nonreciprocal reconfigurable microwave optomechanical circuit, Nat. Commun. **8**, 604 (2017).

[93] Y. Jiang, S. Maayani, T. Carmon, F. Nori, and H. Jing, Nonreciprocal Phonon Laser, Phys. Rev. Appl. **10**, 064037 (2018).

[94] B. J. Li, R. Huang, X.-W. Xu, A. Miranowicz, and H. Jing, Nonreciprocal unconventional photon blockade in a spinning optomechanical system, Photon. Res. **7**, 630 (2019).

[95] J.-H. Liu, Y.-F. Yu, and Z.-M. Zhang, Nonreciprocal transmission and fast-slow light effects in a cavity optomechanical system, Opt. Express **27**, 15382 (2019)

[96] R. Huang, A. Miranowicz, J.-Q. Liao, F. Nori, and H. Jing, Nonreciprocal Photon Blockade, Phys. Rev. Lett. **121**, 153601 (2018).

[97] Q. T. Cao, H. M. Wang, C. H. Dong, H. Jing, R. S. Liu, X. Chen, L. Ge, Q. H. Gong, and Y. F. Xiao, Experimental Demonstration of Spontaneous Chirality in a Nonlinear Microresonator, Phys. Rev. Lett. **118**, 033901 (2017).

[98] L. D. Bino, J. M. Silver, M. T. M. Woodley, S. L. Stebbings, X. Zhao, and P. Del'Haye, Microresonator isolators and circulators based on the intrinsic nonreciprocity of the Kerr effect, Optica **5**, 279 (2018).

[99] Y. Shi, Z. F. Yu, and S. H. Fan, Limitations of nonlinear optical isolators due to dynamic reciprocity, Nat. Photon. **9**, 388 (2015).

[100] L. Fan, J. Wang, L. T. Varghese, H. Shen, B. Niu, Y. Xuan, A. M. Weiner, and M. H. Qi, An all-silicon passive optical diode, Science **335**, 447 (2012).

[101] S. C. Zhang, Y. Q. Hu, G. W. Lin, Y. P. Niu, K. Y. Xia, J. B. Gong, and S. Q. Gong, Thermal-motion-induced nonreciprocal quantum optical system, Nat. Photon. **12**, 744 (2018).

[102] K. Y. Xia, F. Nori, and M. Xiao, Cavity-Free Optical Isolators and Circulators using a Chiral Cross-Kerr Nonlinearity, Phys. Rev. Lett. **121**, 203602 (2018).

[103] K. Wang, Q. Wu, Y.-F. Yu, and Z.-M. Zhang, Nonreciprocal photon blockade in a two-mode cavity with a second-order nonlinearity, Phys. Rev. A **100**, 053832 (2019).

[104] T. Tian, Z. H. Wang, and L. J. Song, Rotation sensing in two coupled whispering-gallery-mode resonators with loss and gain, Phys. Rev. A **100**, 043810 (2019).

[105] C. Caloz, A. Alù, S. Tretyakov, D. Sounas, K. Achouri, and Z.-L. Deck-Léger, Electromagnetic Nonreciprocity, Phys. Rev. Appl. **10**, 047001 (2018).

[106] N. Bender, S. Factor, J. D. Bodyfelt, H. Ramezani, D. N. Christodoulides, F. M. Ellis, and T. Kottos, Observation of Asymmetric Transport in Structures with Active Nonlinearities, Phys. Rev. Lett. **110**, 234101 (2013).

[107] B. Peng, S. K. Özdemir, F. Lei, F. Monifi, M. Gianfreda, G. L. Long, S. H. Fan, F. Nori, C. M. Bender, and L. Yang, Parity-time-symmetric whispering-gallery microcavities, Nat. Phys. **10**, 394 (2014).

[108] L. Chang, X. S. Jiang, S. Y. Hua, C. Yang, J. M. Wen, L. Jiang, G. Y. Li, G. Z. Wang, and M. Xiao, Parity-time symmetry and variable optical isolation in active-passive-coupled microresonators, Nat. Photonics **8**, 524 (2014).

[109] A. Metelmann and A. A. Clerk, Nonreciprocal Photon Transmission and Amplification Via Reservoir Engineering, Phys. Rev. X **5**, 021025 (2015).

[110] D. Malz, L. D. Tóth, N. R. Bernier, A. K. Feofanov, T. J. Kippenberg, and A. Nunnenkamp, Quantum-Limited Directional Amplifiers with Optomechanics, Phys. Rev. Lett. **120**, 023601 (2018).

[111] Z. Shen, Y. L. Zhang, Y. Chen, F. W. Sun, X. B. Zou, G. C. Guo, C. L. Zou, and C. H. Dong, Reconfigurable optomechanical circulator and directional amplifier, Nat. Commun. **9**, 1797 (2018).

[112] P. Lodahl, S. Mahmoodian, S. Stobbe, A. Rauschenbeutel, P. Schneeweiss, J. Volz, H. Pichler, and P. Zoller, Chiral quantum optics, Nature (London) **541**, 473 (2017).

[113] P. D. Nation, J. R. Johansson, M. P. Blencowe, and F. Nori, Colloquium: Stimulating uncertainty: Amplifying the quantum vacuum with superconducting circuits, Rev. Mod. Phys. **84**, 1 (2012).

[114] Z. Leghtas, S. Touzard, I. M. Pop, A. Kou, B. Vlastakis, A. Petrenko, K. M. Sliwa, A. Narla, S. Shankar, M. J. Hatridge, M. Reagor, L. Frunzio, R. J. Schoelkopf, M. Mirrahimi, and M. H. Devoret, Confining the state of light to a quantum manifold by engineered two-photon loss, Science **347**, 853 (2015).

[115] A. F. Adiyatullin, M. D. Anderson, H. Flayac, M. T. Portella-oberli, F. Jabeen, C. Ouellet-Plamondon, G. C. Sallen, and B. Deveaud, Periodic squeezing in a polariton Josephson junction, Nat. Comm. **8**, 1329 (2017).

[116] A. A. Clerk, M. H. Devoret, S. M. Girvin, F. Marquardt, and R. J. Schoelkopf, Introduction to quantum noise, measurement, and amplification, Rev. Mod. Phys. **82**, 1155 (2010).

[117] N. Bartolo, F. Minganti, W. Casteels, and C. Ciuti, Exact steady state of a Kerr resonator with one- and two-photon driving and dissipation: Controllable Wigner-function multimodality and dissipative phase transitions, Phys. Rev. A **94**, 033841 (2016).

[118] F. Minganti, N. Bartolo, J. Lolli, W. Casteels, and C. Ciuti, Exact results for Schrödinger cats in driven-dissipative systems and their feedback control, Sci. Rep. **6**, 26987 (2016).

[119] R. W. Boyd, *Nonlinear Optics* (Academic Press, New York, 2008).

[120] S. T. Shen, Y. Qu, J. H. Li, and Y. Wu, Tunable photon statistics in parametrically amplified photonic molecules, Phys. Rev. A **100**, 023814 (2019)

[121] S. Maayani, R. Dahan, Y. Kligerman, E. Moses, A. U. Hassan, H. Jing, F. Nori, D. N. Christodoulides, and T. Carmon, Flying couplers above spinning resonators generate irreversible refraction, Nature (London) **558**, 569 (2018).

[122] G. B. Malykin, The Sagnac effect: Correct and incorrect explanations, Phys. Usp. **43**, 1229 (2000).

[123] H. K. Shi, Z. F. Xiong, W. J. Chen, J. Xu, S. B. Wang, and Y. T. Chen, Gauge-field description of Sagnac frequency shift and mode hybridization in a rotating cavity, Opt. Express **27**, 28114 (2019).

[124] G. E. Uhlenbeck and L. S. Ornstein, On the theory of the Brownian motion, Phys. Rev. **36**, 823 (1930).

[125] D. T. Gillespie, Exact numerical simulation of the Ornstein-Uhlenbeck process and its integral, Phys. Rev. E **54**, 2084 (1996).

[126] J. Jing and T. Yu, Non-Markovian Relaxation of a Three-Level System: Quantum Trajectory Approach, Phys. Rev. Lett. **105**, 240403 (2010).

[127] H. P. Breuer and F. Petruccione, *The Theory of Open Quantum Systems* (Oxford University Press, Oxford, UK, 2002).

[128] U. Weiss, *Quantum Dissipative Systems*, 3rd ed. (World Scientific, Singapore, 2012).

[129] B. L. Hu, J. P. Paz, and Y. H. Zhang, Quantum Brownian motion in a general environment: Exact master equation with nonlocal dissipation and colored noise, Phys. Rev. D **45**, 2843 (1992).

[130] J. J. Halliwell and T. Yu, Alternative derivation of the Hu-Paz-Zhang master equation of quantum Brownian motion, Phys. Rev. D **53**, 2012 (1996).

[131] G. W. Ford and R. F. O'Connell, Exact solution of the Hu-Paz-Zhang master equation, Phys. Rev. D **64**, 105020 (2001).

[132] H. Z. Shen, S. L. Su, Y. H. Zhou, and X. X. Yi, Non-Markovian quantum Brownian motion in one dimension in electric fields, Phys. Rev. A **97**, 042121 (2018).

[133] M. W. Y. Tu and W. M. Zhang, Non-Markovian decoherence theory for a double-dot charge qubit, Phys. Rev. B **78**, 235311 (2008).

[134] H. Z. Shen, D. X. Li, S. L. Su, Y. H. Zhou, and X. X. Yi, Exact non-Markovian dynamics of qubits coupled to two interacting environments, Phys. Rev. A **96**, 033805 (2017).

[135] H. Z. Shen, X. Q. Shao, G. C. Wang, X. L. Zhao, and X. X. Yi, Quantum phase transition in a coupled two-level system embedded in anisotropic three-dimensional photonic crystals, Phys. Rev. E **93**, 012107 (2016).

[136] H. Z. Shen, D. X. Li, and X. X. Yi, Non-Markovian linear response theory for quantum open systems and its applications, Phys. Rev. E **95**, 012156 (2017).

[137] W. M. Zhang, P. Y. Lo, H. N. Xiong, M. W. Y. Tu, and F. Nori, General Non-Markovian Dynamics of Open Quantum Systems, Phys. Rev. Lett. **109**, 170402 (2012).

[138] H. N. Xiong, W. M. Zhang, X. G. Wang, and M. H. Wu, Exact non-Markovian cavity dynamics strongly coupled to a reservoir, Phys. Rev. A **82**, 012105 (2010).

[139] M. H. Wu, C. U. Lei, W. M. Zhang, and H. N. Xiong, Non-Markovian dynamics of a microcavity coupled to a waveguide in photonic crystals, Opt. Express **18**, 18407 (2010).

[140] C. U. Lei and W. M. Zhang, A quantum photonic dissipative transport theory, Ann. Phys. (NY) **327**, 1408 (2012).

[141] H. Z. Shen, M. Qin, and X. X. Yi, Single-photon storing in coupled non-Markovian atom-cavity system, Phys. Rev. A **88**, 033835 (2013).

[142] K. J. Vahala, Optical microcavities, Nature (London) **424**, 839 (2003).

[143] S. M. Spillane, T. J. Kippenberg, K. J. Vahala, K. W. Goh, E. Wilcut, and H. J. Kimble, Ultrahigh-Q toroidal

microresonators for cavity quantum electrodynamics, Phys. Rev. A **71**, 013817 (2005).

[144] N. G. Pavlov, G. Lihachev, S. Koptyaev, E. Lucas, M. Karpov, N. M. Kondratiev, I. A. Bilenko, T. J. Kippenberg, and M. L. Gorodetsky, Soliton dual frequency combs in crystalline microresonators, Opt. Lett. **42**, 514 (2017).

[145] V. Huet, A. Rasoloniaina, P. Guillemé, P. Rochard, P. Féron, M. Mortier, A. Levenson, K. Bencheikh, A. Yacomotti, and Y. Dumeige, Millisecond Photon Lifetime in a Slow-Light Microcavity, Phys. Rev. Lett. **116**, 133902 (2016).

[146] J. A. Zielińska and M. W. Mitchell, Self-tuning optical resonator, Opt. Lett. **42**, 5298 (2017).

[147] R. Reimann, M. Doderer, E. Hebestreit, R. Diehl, M. Frimmer, D. Windey, F. Tebbenjohanns, and L. Novotny, GHz Rotation of an Optically Trapped Nanoparticle in Vacuum, Phys. Rev. Lett. **121**, 033602 (2018).

[148] J. Ahn, Z. Xu, J. Bang, Y.-H. Deng, T. M. Hoang, Q. Han, R. M. Ma, and T. Li, Optically Levitated Nanodumbbell Torsion Balance and GHz Nanomechanical Rotor, Phys. Rev. Lett. **121**, 033603 (2018).

[149] B. Coutinho dos Santos, K. Dechoum, A. Z. Khoury, L. F. da Silva, and M. K. Olsen, Quantum analysis of the nondegenerate optical parametric oscillator with injected signal, Phys. Rev. A **72**, 033820 (2005).

[150] D. F. Walls and G. J. Milburn, *Quantum Optics* (Springer, Berlin, 1994).

[151] C. Gerry and P. Knight, *Introductory Quantum Optics* (Cambridge University Press, Cambridge, 2005).

[152] W. Qin, A. Miranowicz, P. B. Li, X. Y. Lü, J.-Q. You, and F. Nori, Exponentially Enhanced Light-Matter Interaction, Cooperativities, and Steady-State Entanglement using Parametric Amplification, Phys. Rev. Lett. **120**, 093601 (2018).

[153] M. Notomi, Manipulating light with strongly modulated photonic crystals, Rep. Prog. Phys. **73**, 096501 (2010).

[154] J. T. Robinson, C. Manolatou, L. Chen, and M. Lipson, Ultrasmall Mode Volumes in Dielectric Optical Microcavities, Phys. Rev. Lett. **95**, 143901 (2005).

[155] S. Bergfeld and W. Daum, Second-Harmonic Generation in GaAs: Experiment versus Theoretical Predictions of $\chi^{(2)}_{xyz}$, Phys. Rev. Lett. **90**, 036801 (2003).

[156] S. Combrié, A. De Rossi, N. Q. V. Tran, and H. Benisty, GaAs photonic crystal cavity with ultrahigh Q: Microwatt nonlinearity at 1.55 μm, Opt. Lett. **33**, 1908 (2008).

[157] H. Z. Shen, S. Xu, H. T. Cui, and X. X. Yi, Non-Markovian dynamics of a system of two-level atoms coupled to a structured environment, Phys. Rev. A **99**, 032101 (2019).

[158] H. Z. Shen, S. Xu, S. Yi, and X. X. Yi, Controllable dissipation of a qubit coupled to an engineering reservoir, Phys. Rev. A **98**, 062106 (2018).

[159] T. Shi, Y.-H. Wu, A. Gonzlez-Tudela, and J. I. Cirac, Bound States in Boson Impurity Models, Phys. Rev. X **6**, 021027 (2016).

[160] T. Shi, Y.-H Wu, A. González-Tudela, and J. I. Cirac, Effective many-body Hamiltonians of qubit-photon bound states, New J. Phys. **20**, 105005 (2018).

[161] G. Calajó and P. Rabl, Strong coupling between moving atoms and slow-light Cherenkov photons, Phys. Rev. A **95**, 043824 (2017).

[162] T. Shi, Y. Chang, and J. J. García-Ripoll, Ultrastrong Coupling Few-Photon Scattering Theory, Phys. Rev. Lett. **120**, 153602 (2018).

[163] L. Lo and C. K. Law, Quantum radiation from a shaken two-level atom in vacuum, Phys. Rev. A **98**, 063807 (2018).

[164] W. Z. Zhang, J. Cheng, W. D. Li, and L. Zhou, Optomechanical cooling in the non-Markovian regime, Phys. Rev. A **93**, 063853 (2016).

[165] W. Z. Zhang, Y. Han, B. Xiong, and L. Zhou, Optomechanical force sensor in a non-Markovian regime, New J. Phys. **19**, 083022 (2017).

[166] J. F. Triana, A. F. Estrada, and L. A. Pachón, Ultrafast Optimal Sideband Cooling under Non-Markovian Evolution, Phys. Rev. Lett. **116**, 183602 (2016).